available at www.sciencedirect.com

ScienceDirect

www.elsevier.com/locate/brainres

BRAIN RESEARCH

Research Report

Morphological variability of NADPH diaphorase neurons across areas V1, V2, and V3 of the common agouti

Marco Aurélio M. Freire[a,b,1], *Emiliana G. Rocha*[a,1], *Jorge Luiz F. Oliveira*[a], *Joanilson S. Guimarães*[a,e], *Luiz Carlos L. Silveira*[c,d], *Guy N. Elston*[f], *Antonio Pereira*[a,e,*,1], *Cristovam W. Picanço-Diniz*[a,1]

[a]*Lab. Neurodegeneração e Infecção, Hospital Universitário João de Barros Barreto, Universidade Federal do Pará, 66073-000 Belém, PA, Brazil*
[b]*Universidade Potiguar, 59056-000 Natal, RN, Brazil*
[c]*Lab. Neurofisiologia Eduardo Oswaldo-Cruz, Instituto de Ciências Biológicas, Universidade Federal do Pará, 66075-900 Belém, PA, Brazil*
[d]*Lab. Neurologia Tropical, Núcleo de Medicina Tropical, Universidade Federal do Pará, 66055-240 Belém, PA, Brazil*
[e]*The Edmond and Lily Safra International Institute of Neuroscience of Natal (ELS-IINN), 59066-060 Natal, RN, Brazil*
[f]*Centre for Cognitive Neuroscience, Sunshine Coast, Queensland 4562, Australia*

ARTICLE INFO

Article history:
Accepted 14 December 2009
Available online 28 December 2009

Keywords:
Interneuron
Striate
Extrastriate
Area 17
Area 18
Rodent

ABSTRACT

Previous studies have shown a noticeable phenotypic diversity for pyramidal cells among cortical areas in the cerebral cortex. Both the extent and systematic nature of this variation suggests a correlation with particular aspects of cortical processing. Nevertheless, regional variations in the morphology of inhibitory cells have not been evaluated with the same detail. In the present study we performed a 3D morphometric analysis of 120 NADPH diaphorase (NADPH-d) type I neurons in the visual cortex of a South American Hystricomorph rodent, the diurnal agouti (*Dasyprocta* sp.). We found significant differences in morphology of NADPH-d type I neurons among visual cortical areas: cells became progressively larger and more branched from V1 to V2 and V3. Presumably, the specialized morphology of these cells is correlated with different sampling geometry and function. The data suggest that area-specific specializations of cortical inhibitory circuitry are also present in rodents.

1. Introduction

Recent studies in primates have revealed a marked degree of morphological specialization of neuronal circuits across different cortical areas. Pyramidal cells, which comprise more than 70% of the neurons in the cerebral cortex (DeFelipe and Farinas, 1992), differ in size, branching pattern, and number of dendritic spines in different cortical areas (Elston, 2002; Elston, 2003a; Jacobs and Scheibel, 2002). Interneurons, which comprise most of the remaining neurons, also differ in their morphology in distinct cortical areas (DeFelipe et al., 1999; Gabbott et al., 1997; Lund et al., 1993). Moreover, systematic trends in circuit specialization have been documented in homologous cortical pathways in different species:

* *Corresponding author*. Edmond and Lily Safra International Institute of Neuroscience of Natal (ELS-IINN), Rua Prof. Francisco Luciano de Oliveira 2460, 59066-060 Natal, RN, Brazil.
E-mail address: apereira@ufrnet.br (A. Pereira).
[1] Contributed equally to this work.

0006-8993/$ – see front matter © 2009 Elsevier B.V. All rights reserved.
doi:10.1016/j.brainres.2009.12.045

the dendritic trees of neurons tend to become more spinous with increasing functional complexity along the pathway (see Elston, 2007 for a review).

To date, few systematic quantitative studies have been performed in the rodent cerebral cortex (e.g., Benavides-Piccione et al., 2006). In fact, much of the earlier work performed in rodent species led to the theory of cortical uniformity (e.g., Szentagothai, 1975). This theory, however, has been subjected to intense scrutiny (e.g., Barone and Kennedy, 2000; Elston, 2002, 2003a; Jacobs and Scheibel, 2002). Advances in our understanding of the brain over the last four decades suggest that a re-examination of the organization of the rodent cerebral cortex is required to better understand species specializations and evolutionary trends (see Kaas, 2005; Krubitzer, 2009; Preuss, 2000 for reviews). Here we focus our attention on the agouti, a diurnal Hystricomorph with several species belonging to the single genus Dasyprocta. The agouti is native to tropical America and has a medium-sized body (about 3.5 kg). Its visual system has been the subject of several studies, including eye optics (Oswaldo-Cruz et al., 1985), photoreceptor (Rocha et al., 2009), horizontal (de Lima et al., 2005), and retinal ganglion cell topography (Gomes et al., 1998; Silveira et al., 1989), visual cortex anatomy (Costa et al., 1996; Elston et al., 2006; Picanço-Diniz et al., 1989; Picanço-Diniz et al., 1992) and physiology (Picanço-Diniz et al., 1991; Picanço-Diniz et al., 1992). The agouti has a large lisencephalic brain, which is well suited for mapping studies (Picanço-Diniz et al., 1989; Rocha et al., 2007; see Santiago et al., 2007 for details) (Fig. 1). As befits a diurnal species, the agouti is a highly visual rodent, with a prominent visual streak in the retina (Silveira et al., 1989) and a well developed visual cortex including at least 3 distinguishable areas: the primary (V1), second (V2) and third (V3) visual areas (Picanço-Diniz et al., 1989; Picanço-Diniz et al., 1991).

Recently, we demonstrated that a class of excitatory neurons, the pyramidal cells, become increasingly larger, more branched, and with more dendritic spines across V1, V2 and V3 in the agouti (Elston et al., 2006), consistent with observations in monkeys (Elston et al., 1999a,b). So far, however, no one has performed a systematic quantitative comparison of inhibitory neurons within these areas. In the present work, we quantified the morphology of a subpopulation of inhibitory cells, the nitrergic neurons (Vincent and Kimura, 1992). This cell group can be readily detected by a simple histochemical reaction that uses the enzyme nicotinamide adenine dinucleotide phosphate diaphorase (NADPH-d) (Thomas and Pearse, 1964), which reveals two sub-types of cells according to their morphological characteristics (Freire et al., 2005; Luth et al., 1994). Type I neurons have larger cell bodies, more ramified dendritic trees, and are more reactive than type II neurons (Luth et al., 1994). Although the morphology of NADPH-d type I neurons has been evaluated in a number of species in both normal and altered conditions (Franca et al., 2000; Freire et al., 2004, 2007, 2008; Norris et al., 1996; Pereira et al., 2000; Sandell, 1986; Tao et al., 1999; Yan and Garey, 1997), we are unaware of any study in which the morphology of these neurons has been quantified and compared systematically amongst functionally related cortical areas. Thus, we reconstructed NADPH-d type I neurons in 3D and studied how their morphology varies across areas V1, V2, and V3. We have found that similar to pyramidal cells, NADPH-d type I neurons become increasingly larger and more ramified when one moves from V1 to V2 and V3, suggesting the existence of a specialized inhibitory circuitry across visual cortical areas of this species.

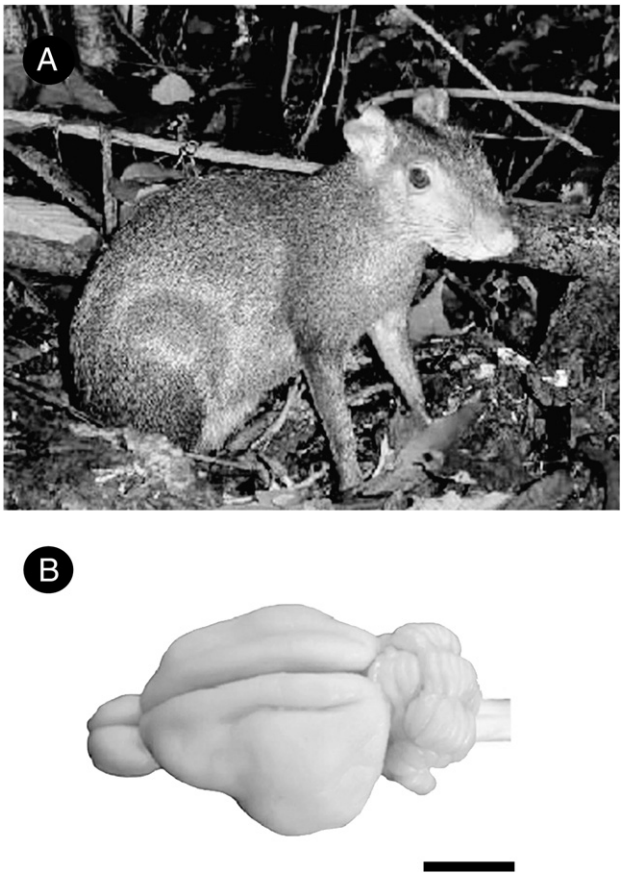

Fig. 1 – The agouti (*Dasyprocta sp.*) (A), assuming a typical vigilant posture. (B) A dorsolateral view of its lisencephalic brain. Scale bar: 1 cm.

2. Results

2.1. *Reactivity of NADPH-d in the visual cortex*

Figure 2 shows a tangential section of the flattened agouti cortex, reacted for NADPH-d, with the limits of different visual areas being distinctly identifiable. Notice the primary visual area (V1) (adjacent to and extending underneath to the lateral sulcus), the second visual area (V2) and the adjacent third visual area (V3). The location and boundaries of visual areas revealed by NADPH-d are similar to those previously determined by electrophysiological mapping, cytoarchitecture, and patterns of myelination (Elston et al., 2006; Picanço-Diniz et al., 1989).

Since the limits of visual areas were precisely defined with the NADPH-d histochemistry, we were able to determine with precision the identity of cortical areas from which individual

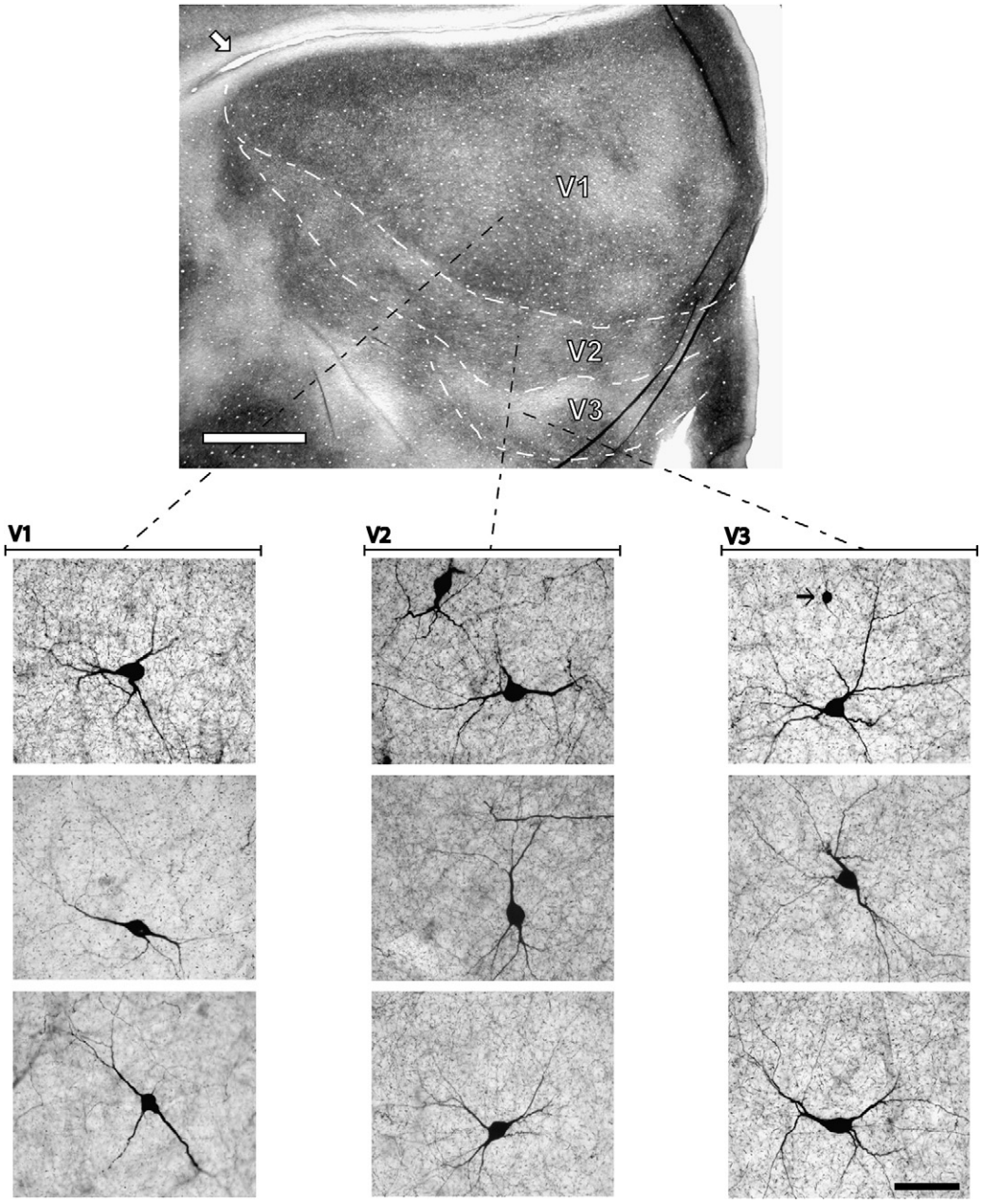

Fig. 2 – Tangential section of the agouti's left brain hemisphere processed for NADPH-d histochemistry. Notice the location of the primary visual area (V1) adjacent to and extending underneath the lateral sulcus (arrow), the second visual area (V2) and the adjacent third visual area (V3). The photomicrographs below illustrate select NADPH-d positive neurons in each cortical area. The arrow points to a type II neuron located in the area V3. Scale bars: 2 mm (lower magnification); 100 μm (enlargements).

NADPH-d type I neurons were being sampled. We observed a wide diversity in both cell body size and dendritic morphology of cells across areas, including multipolar, stellate, and bipolar cell morphology (Fig. 2). Fig. 3 shows representative examples of neurons from different visual areas with information about cell body size (Cb), dendritic field area (Df), and fractal dimension (D).

2.2. *Analysis by cortical area*

Based on neuron location within cortical areas V1, V2 and V3, a total of 120 NADPH-d type I neurons were selected for analyses (Tables 1 and 2). Comparison among these cells revealed that the size of cell bodies became progressively larger from V1 ($379.51 \pm 11.17\ \mu m^2$) to V2 ($407.44 \pm 12.34\ \mu m^2$) ($F_{2,87} = 10.48$) and V3 ($428.57 \pm 10.27\ \mu m^2$) ($F_{2,87} = 1.73$) (Fig. 4A). While an ANOVA revealed these differences to be significant ($p < 0.01$), a *post-hoc* Newman–Keuls test revealed a significant difference only between V1 and V3, but not between V1 and V2 or between V2 and V3. The dendritic trees of NADPH-d type I neurons also became increasingly larger from V1 ($47.89 \pm 2.02 \times 10^3\ \mu m^2$), to V2 ($68.28 \pm 2.03 \times 10^3\ \mu m^2$), and V3 ($83.30 \pm 1.90 \times 10^3\ \mu m^2$) ($F_{2,87} = 32.88$) (Fig. 4B). A *post-hoc* Newman–Keuls test revealed that all pair-wise comparisons

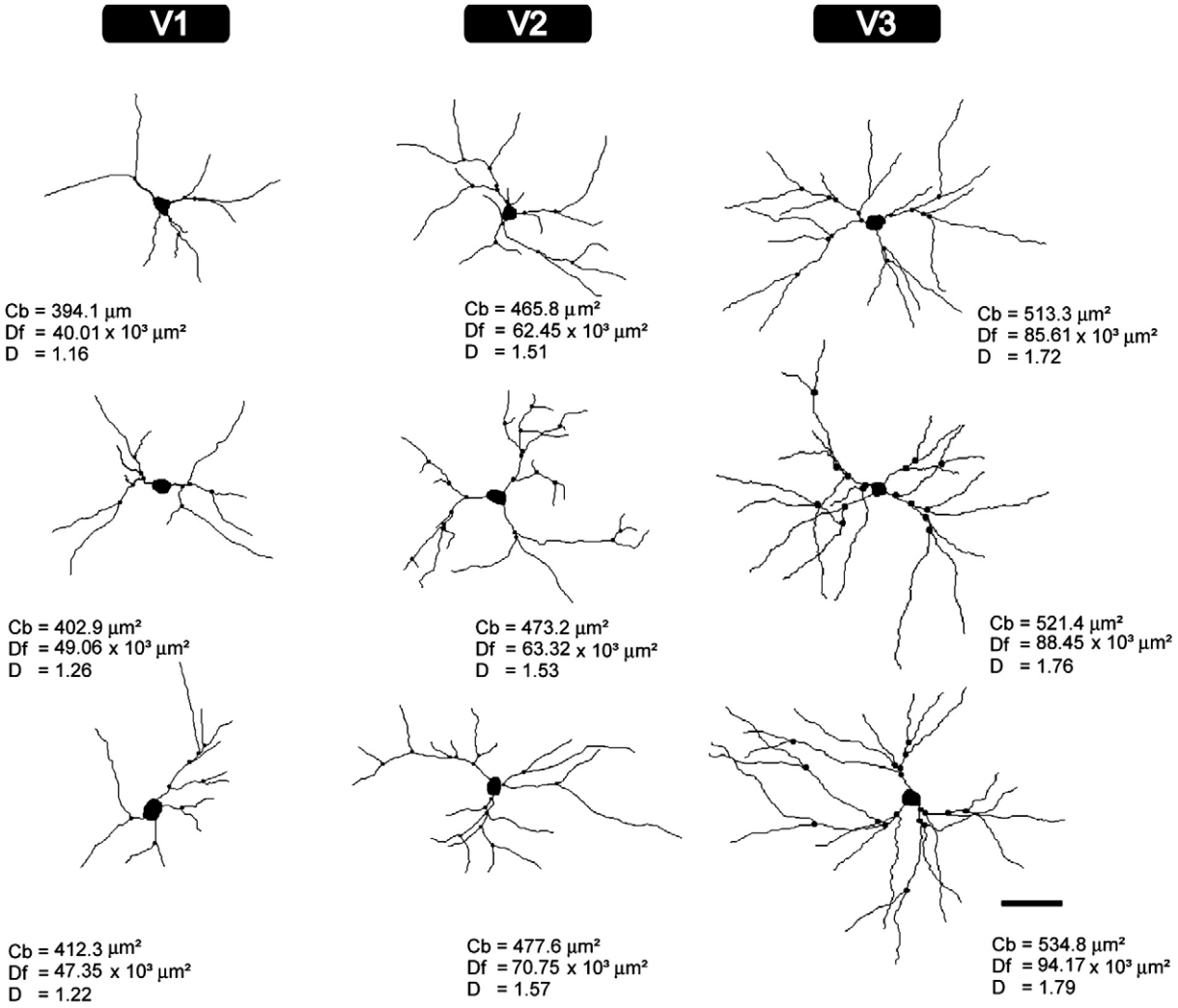

Fig. 3 – Examples of reconstructed cells from primary (V1), second (V2) and third (V3) visual areas. The size of the cell body (Cb), the dendritic field area (Df) and the fractal dimension (D, dilation method) is given for each cell. Scale bar: 100 µm.

were significant ($p<0.05$). In addition, cells in V1 had fewer ramifications than those in V2 and V3, with the latter being more ramified than both V1 and V2 neurons (Fig. 4B,C). The maximum degree of ramification occurred in third order dendrites for all groups. Likewise, fractal analyses revealed that the branching pattern of NADPH-d cells became progressively more complex from V1 (dilation: 1.347±0.011; mass radius: 1.414±0.017), to V2 (dilation: 1.402±0.012; mass radius: 1.462±0.014) ($F_{1,58}=23.75$—dilation; $F_{1,58}=19.09$—mass radius) and V3 (dilation: 1.451±0.018; mass radius: 1.517±0.017) ($F_{2,87}=4.98$—dilation; $F_{2,87}=6.34$—mass radius) (Figs. 4D–E). For each method (dilation and mass radius), the *post-hoc* Newman–Keuls test revealed that all pair-wise comparisons were significant ($p<0.05$).

Table 1 – Size of the cell bodies (µm²) and dendritic trees (x10³ µm²) of NADPH-d neurons across visual areas.

Visual area	Mean	SD	SEM	Minimum	Maximum
Cell body					
V1	379.51	61.1	11.17	277.40	545.90
V2	407.44	67.5	12.34	263.10	534.30
V3	428.57	56.2	10.27	292.40	523.20
Dendritic field					
V1	47.89	12.35	2.02	29.71	67.00
V2	68.28	17.41	2.03	41.45	85.52
V3	83.30	18.41	1.90	60.79	98.08

Table 2 – Fractal dimension (dilatation and mass radius) of NADPH-d neurons across visual areas.

Visual area	Mean	SD	SEM	Minimum	Maximum
Fractal analysis (dilation)					
V1	1.347	0.060	0.011	1.252	1.468
V2	1.402	0.066	0.012	1.279	1.547
V3	1.451	0.099	0.018	1.269	1.665
Fractal analysis (mass radius)					
V1	1.414	0.091	0.017	1.292	1.536
V2	1.462	0.079	0.014	1.314	1.653
V3	1.451	0.092	0.017	1.311	1.679

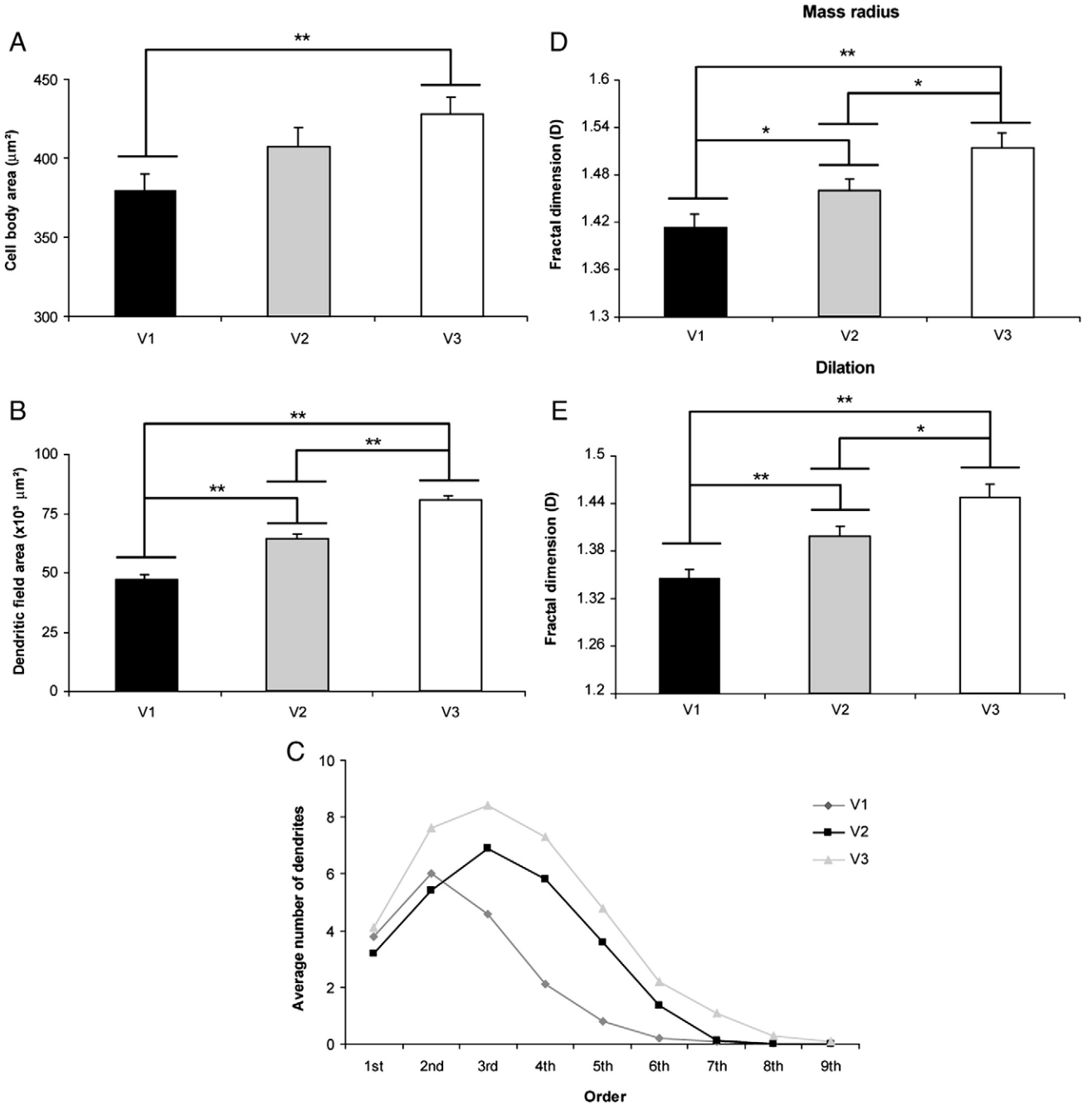

Fig. 4 – Histograms comparing key quantitative morphological parameters from NADPH-d type I neurons in the primary (V1), second (V2) and third (V3) visual areas of the agouti. There is a progressive increase in the size of the cell bodies (A), the dendritic field area (B), the number of dendrites (C) and the fractal dimension (D and E) from V1 to V2 and V3. Horizontal bars show significant differences according to the Newman–Keuls *post-hoc* test ($^{*}p<0.05$ and $^{**}p<0.01$).

2.3. *Cluster analysis of neuronal morphology*

In addition to the comparative analysis of morphological parameters of NADPH-d type I neurons according to which cortical area they belonged to, we performed a cluster analysis of all 120 neurons. A multivariate analysis separated three distinct groups of cells, with neurons from each cortical area tending to be clustered together (Fig. 5). When comparing V1 and V2 neurons, for instance, we noticed a less defined clustering of V1 neurons (Fig. 5, top tree). Likewise, when comparing V1 and V3, only 8 neurons from the former clustered together, while 4 of V3 neurons clustered with the

Fig. 5 – Dendrograms generated from cluster analysis of morphometrical parameters of all neurons pooled from V1, V2 and V3. Neurons are identified by labels at the bottom of each tree branch.

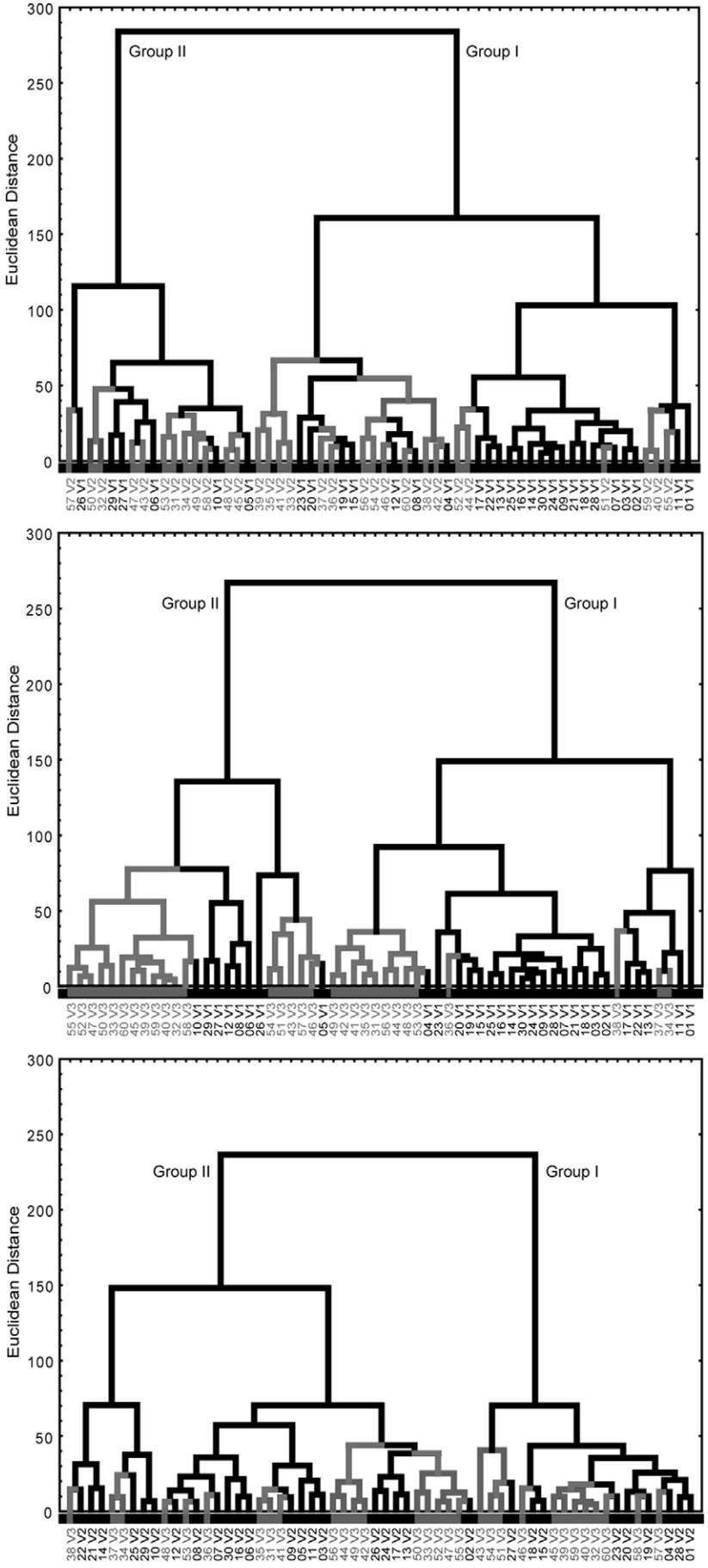
Group II
Group I
Euclidean Distance
300
250
200
150
100
50
0

V1 group (Fig. 5, middle tree). In V2 and V3 clusters, 9 neurons from V3 clustered with V2, while 10 neurons from V1 shared a cluster with V3 (Fig. 5, bottom tree).

3. Discussion

In the present study we quantified the morphology of NADPH-d type I neurons in the agouti's cortical areas V1, V2, and V3. We found that the boundaries of all three cortical areas revealed by NADPH-d histochemistry were consistent with those revealed previously by both electrophysiological mapping (Picanço-Diniz et al., 1989) and cytochrome oxidase histochemistry (Elston et al., 2006). A comparison of the morphology of dendritic trees of NADPH-d type I neurons revealed that they become more complex with lateral progression through areas V1, V2 and V3.

3.1. *Neuropil reactivity and nitrergic neurons of the agouti visual cortex*

The NADPH-d reactive neuropil allows one to define with precision the boundaries between visual areas not only in the agouti but also in other distantly related species (see Franca et al., 2000), although the reasons for the existence of compartments with high and low enzymatic activity remains to be fully clarified. In layer IVC of the monkey's visual cortex, for instance, there is also a high concentration of dispersed NOS/NADPH-d neuropil but few reactive cell profiles (Franca et al., 1997). Using electron microscopy reconstructions Aoki et al. (1993) demonstrated that NOS-immunoreactive neuropil in V1 corresponds predominantly to presynaptic terminals of unknown origin. Since NADPH-d/NO is directly correlated to metabolism in the primate brain (Wong-Riley et al., 1998) it can actively regulate neuronal activity.

After the discovery that NO is a NADPH-d in the 1990s, histochemical methods that reveal NADPH-d activity were applied to identify NO-producing neurons (Dawson et al., 1991; Hope et al., 1991). NO is a highly diffusible molecule that is involved in several physiological and pathological events in the nervous system (see Calabrese et al., 2007; Freire et al., 2009; Guimarães et al., 2009 for reviews). Accordingly, NADPH-d neurons could contribute, for instance, to the regulation of the cerebral microvasculature through NO (Estrada and DeFelipe, 1998).

3.2. *Homogeneity vs. heterogeneity in the neocortex*

There are two opposing theories related to the microstructure of the mammalian cerebral cortex. One theory posits that the neocortex is composed of repeated columns of cells each of which comprises a canonical circuit (Binzegger et al., 2004; Douglas et al., 1989; Mountcastle, 1997). The other theory states that neuronal structure and patterns of connectivity vary greatly across the cortical mantle (Elston, 2007; Horton and Adams, 2005; Jacobs and Scheibel, 2002; Nelson, 2002). The present data are consistent with the latter view: the morphology of NADPH-d type I neurons differ significantly amongst cortical areas. The dendritic trees of NADPH-d type I cells in V3 were, on average, about 75% larger than those in V1. The dendritic trees of these cells in V3 were, on average, 50% more branched than those in V1. In addition, as reported previously in the visual cortex of primates (Barone and Kennedy, 2000; Elston, 2003b; Elston et al., 2005a,b,c 1999a,b), neuronal morphology differed systematically among functionally related cortical areas. The dendritic trees of neurons become increasingly larger and more branched with increasing cortical hierarchy. How then might these specializations in neuronal morphology influence function?

3.3. *Functional implications of specialized morphologies*

As reviewed in detail elsewhere, differences in the size and branching complexity of dendritic trees may influence the computational capability of neurons at the subcellular and cellular level (Elston, 2003a; Jacobs and Scheibel, 2002; Spruston, 2008). For example, the relationship between the size of the dendritic tree of NADPH-d type I neurons and the size of the topographic map in a given area could determine the proportion of the visuotopic representation over which the cell may exert a direct influence (Lund et al., 1993; Malach, 1994). This potential influence is magnified as the size of the visuotopic map is increasingly reduced from V1 to V2, and V3, while dendritic trees become progressively larger. Differences in the number of branches in the dendritic tree influence their space-filling capacity and may determine the potential to compartmentalize the processing of inputs (Elston, 2003a; Jelinek et al., 2005; Mel, 1999; Rall et al., 1992; Segev, 1998; Spruston et al., 1999; Stuart et al., 1997). Differences in the number of branches in the dendritic tree may also influence the decay of backpropagating potentials, believed to be important in the Hebbian reinforcement of inputs and their distribution (Elston and DeFelipe, 2002; Vetter et al., 2001).

Differences in total dendritic length influence the electrotonic properties of neurons as well (Mainen and Sejnowski, 1996; Rall, 1959, 1989; Rothnie et al., 2006). Moreover, the potential differences in the distribution of inputs throughout the dendritic trees, and the spatial configuration of the dendritic tree have been shown to influence both the functional capacity of neurons and the memory storage

Fig. 6 – Illustration of methods used to determine (A) the size of both the dendritic trees and cell bodies; (B) their branching profile (Sholl analysis); and (C) their space filling capacity (fractal dimension). The size of the dendritic trees was calculated as the area contained within a polygon formed by joining the distal dendritic tips, while cell body size was determined as the area determined by the cell body profile (arrow), excluding the parent dendrite expansions. Branching complexity was determined by Sholl analyses. The space filling (fractal dimension) was calculated by reducing the thickness of the dendrites to one pixel (Ai). Circles of increasing diameter were drawn over each pixel along the skeletonized dendrites (Aii-iv) and the percentage coverage within the dendritic tree was calculated. We repeated the process 26 times and the resulting data was plotted (B). We removed outliers from the data set (colored dots) and the fractal value (D) was calculated.

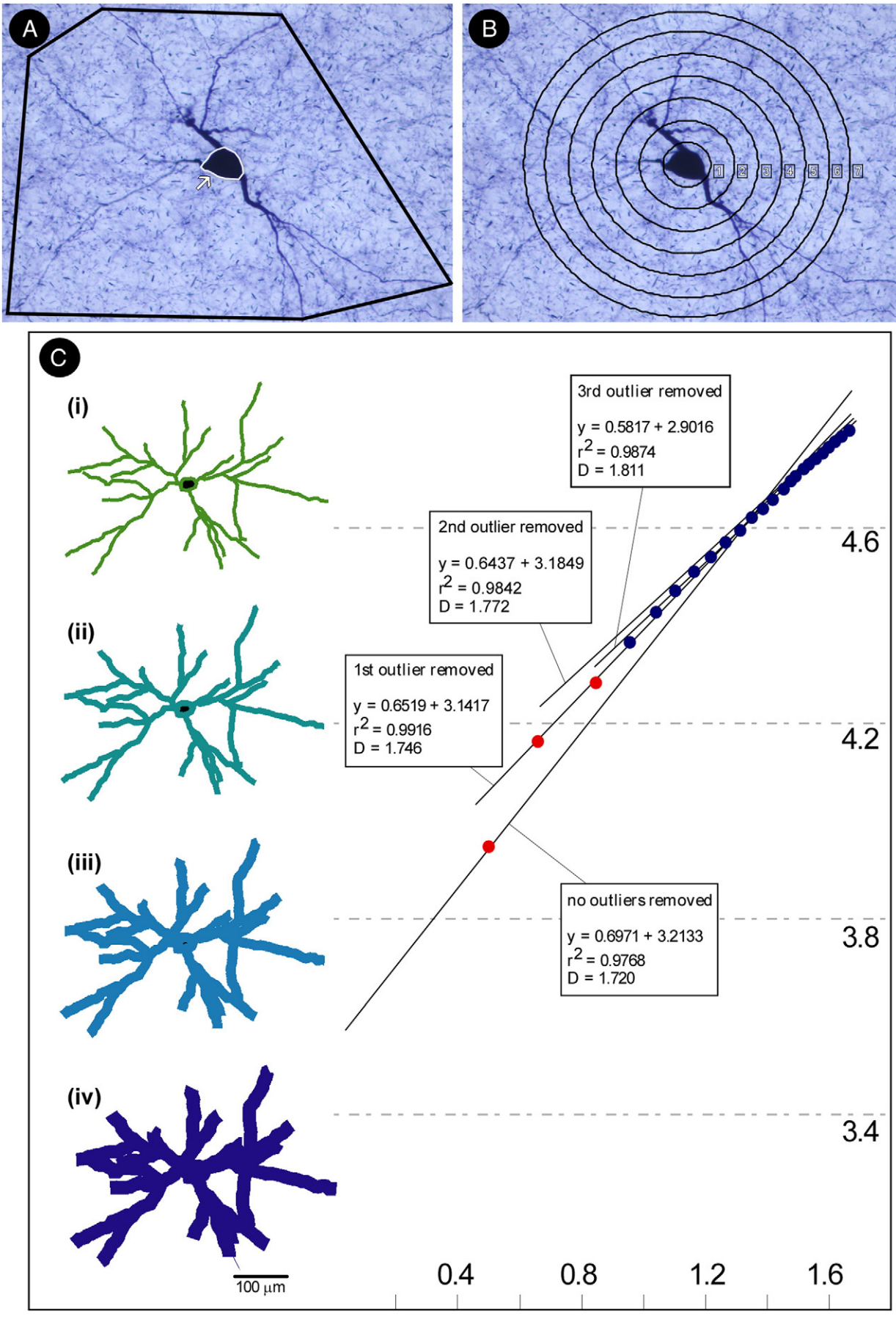
A
B
C
(i)
(ii)
(iii)
(iv)
3rd outlier removed
y = 0.5817 + 2.9016
r2 = 0.9874
D = 1.811
2nd outlier removed
y = 0.6437 + 3.1849
r2 = 0.9842
D = 1.772
1st outlier removed
y = 0.6519 + 3.1417
r2 = 0.9916
D = 1.746
no outliers removed
y = 0.6971 + 3.2133
r2 = 0.9768
D = 1.720
4.6
4.2
3.8
3.4
0.4
0.8
1.2
1.6
100 μm

capacity of cortical circuits they comprise (Poirazi and Mel, 2001; Stepanyants et al., 2002). Further electrophysiological mapping studies will be required to provide the empirical data to reveal how structural differences in NADPH-d type I neurons reported here may influence their function.

3.4. *On cell body size and the dendritic tree*

The present results suggest that cell body size is correlated with both the size of the dendritic trees and the complexity of their branching structure. Studies in the visual cortex of primates reveal a similar trend (Elston and Rosa, 1998; Elston et al., 1999a; Elston et al., 2005a–c). However, similar comparisons in other cortical regions revealed a lack of correlation between cell body size and either the size of the dendritic trees or their branching complexity (Elston and Rockland, 2002). For example, there was only a 50% correspondence between cell body size and the size of the dendritic trees of neurons in the sensorimotor cortex of macaque monkey (Elston and Rockland, 2002). Other comparisons also revealed a lack of consistency between cell body size and the size of dendritic trees. For example, soma size is significantly different between cells in areas 4 and 5 of the macaque monkey, but there is no significant difference in the size of their dendritic trees. In fact, comparison of some populations of neurons reveals a reverse correlation; namely, the larger the cell body the smaller the dendritic tree (Elston and Rosa, 2006). Moreover, even when there is no significant difference in the size of the cell somata in different cortical areas, there may be marked differences in the number of spines contained within their dendritic trees: cells in area 6 of the macaque monkey contain at least 75% more spines than those in areas 4 and 5, but their somata are not significantly different in size (Elston and Rockland, 2002). Various other groups have also reported a lack of correlation between the size of the cell body of cortical neurons and the structure of their dendritic trees (rat somatosensory cortex: Larkman, 1991a,b; cat visual cortex: Matsubara et al., 1996) suggesting widespread variance between these parameters.

4. Conclusion

We have shown that the dendritic trees of NADPH-d type I neurons differ among cortical areas V1, V2 and V3 of the agouti. Cells increased systematically in both size and branching complexity with progression from V1 to V2 and V3. Thus, there appears to be a systematic increase in input-sampling convergence at progressively higher levels along the cortical visual pathway. These data, taken together with those reported elsewhere for pyramidal cells (Benavides-Piccione et al., 2006; Elston et al., 2006) suggest that systematic specialization in cortical circuitry may be common in the rodent cerebral cortex. Nonetheless, as NADPH neurons constitute only a small proportion of inhibitory interneurons (Gonchar and Burkhalter, 1997; DeFelipe et al., 1999; Gonzalez-Albo et al., 2001), it will be worthwhile in future studies to compare the morphology of other types of interneurons to better comprehend the extent of specialization of inhibitory circuitry among cortical areas.

5. Experimental procedures

5.1. *Perfusion, tissue preparation and histochemical processing*

Five adult male agoutis (*Dasyprocta* sp.), obtained from the Federal University of Pará central animal facility were used in the present study. The animals were deeply anaesthetized with urethane (1.25 mg/kg, *i.p.*) or a mixture of ketamine (10 mg/kg, *i.p.*) and xylazine (1 mg/kg, *i.p.*) and perfused transcardially with 0.9% heparinized-saline, followed by 4% paraformaldehyde (Sigma Company, St Louis, MO, USA) in 0.1 M phosphate buffer (PB), pH 7.4. All experimentation was performed in accordance with guidelines from the Brazilian Institute of the Environment and Renewable Natural Resources (IBAMA) (license 207419-0030/2003) and the NIH Guide for the Care and Use of Laboratory Animals.

The brains were removed from the skull, the tissue was flattened between two glass slides (immersed in 0.1 M PB overnight) and then cut tangentially at 200 μm with a Vibratome (Pelco International, Series 1000). For the NADPH-d histochemistry (*indirect* method, modified from Scherer-Singler et al., 1983), all sections were reacted free floating as follows: the tissue was incubated in a solution containing 0.6% malic acid, 0.03% nitroblue tetrazolium, 1% dimethylsulfoxide, 0.03% manganese chloride, 0.5% β-NADP and 1.5-3% Triton X-100 in 0.1 M Tris buffer, pH 8.0. The reaction was monitored every 30 min to avoid overstaining and was interrupted by rinsing sections in Tris buffer (pH 8.0) when well-stained secondary and tertiary dendrites of NADPH-d cells could be visualized at lower magnification. Sections were then mounted onto gelatinized-glass slides, air-dried overnight, dehydrated through a series of graded alcohols and cover-slipped with Entellan (Merck, Germany). All reagents were purchased from Sigma Company, USA.

Sections were photographed prior to, and after, processing to allow correction factors to be applied for any shrinkage. If a section was estimated to have reduced in size by 2% during processing, the size of the dendritic trees, for example, was adjusted in the reported data to correct for this artifact. Moreover, neurons were sampled from V1, V2 and V3 within any given section. As there was no estimable difference in shrinkage among these cortical areas it is unlikely that the difference in the size of the dendritic trees we report here among cortical areas could be attributed to different shrinking with batch processing, for example.

5.2. *Delineation of cortical areas*

The boundaries of cortical areas V1, V2 and V3 have been determined by electrophysiological mapping, cytoarchitecture, and patterns of myelination (Elston et al., 2006; Picanço-Diniz et al., 1989). Moreover, the temporal posterior area (TP) with visually responsive neurons has also been identified lateral to V3 lateral border. In the present work, we have defined them in tangential sections processed for NADPH-d histochemistry. Thus, we were able to determine with accuracy from which cortical areas we sampled individual NADPH-d type I neurons. Since the general pattern of tissue

reactivity defining visual limits is restricted to layer IV, we were confident we have sampled all neurons from this layer, normally encompassed in three sections.

5.3. *Neuronal reconstructions, qualitative and quantitative analysis*

We reconstructed a total of 120 NADPH-d type I neurons in 3D while viewed through an oil immersion lens (60× planapochromatic objective) coupled with an Optiphot-2 microscope (Nikon, Tokyo, Japan) equipped with a motorized stage (MAC200, LUDL, Hawthorne, NY, USA) and a computer running the *Neurolucida* software (MBF Bioscience, Williston, VT, USA). We selected 40 neurons randomly from each cortical area (about 8–10 cells per animal, throughout three sections). Only neurons that had the entire dendritic arborization placed within a single section were included for analyses. Four morphometric parameters were evaluated: (1) area of dendritic arborization, in μm^2 (the area defined by the polygon joining the outermost distal tips of the dendrites; Fig. 6A); (2) area of cell body (Fig. 6A, arrow); (3) number of dendrites by order (Fig. 6B); and (4) fractal dimension (*D*)—including that derived by the dilation and mass radius methods (Fig. 6C; see Jelinek et al., 2005 for details). All measurements were made with the *Neuroexplorer* software (MBF Bioscience). Cluster analysis was performed using these parameters (Schweitzer and Renehan, 1997).

Comparisons between different groups were made by analysis of variance (ANOVA) with the Newman–Keuls *post hoc* test. Significance level was preset at 95% ($p<0.05$). All values are reported as mean±standard error of mean (SEM).

Acknowledgments

This research was supported by grants from Conselho Nacional de Desenvolvimento Científico e Tecnológico (CNPq) #486351/2006-8, #620248/2006-8, #620037/2008-3, and Financiadora de Estudos e Projetos (FINEP) "Rede Instituto Brasileiro de Neurociência (IBN-Net)" #01.06.0842-00. AP, LCLS and CWPD are CNPq research fellows.

REFERENCES

Aoki, C., Fenstemaker, S., Lubin, M., Go, C.G., 1993. Nitric oxide synthase in the visual cortex of monocular monkeys as revealed by light and electron microscopic immunocytochemistry. Brain Res. 620, 97–113.

Barone, P., Kennedy, H., 2000. Non-uniformity of neocortex: areal heterogeneity of NADPH-diaphorase reactive neurons in adult macaque monkeys. Cereb. Cortex 10, 160–174.

Benavides-Piccione, R., Hamzei-Sichani, F., Ballesteros-Yanez, I., DeFelipe, J., Yuste, R., 2006. Dendritic size of pyramidal neurons differs among mouse cortical regions. Cereb. Cortex 16, 990–1001.

Binzegger, T., Douglas, R.J., Martin, K.A., 2004. A quantitative map of the circuit of cat primary visual cortex. J. Neurosci. 24, 8441–8453.

Calabrese, V., Mancuso, C., Calvani, M., Rizzarelli, E., Butterfield, D.A., Stella, A.M., 2007. Nitric oxide in the central nervous system: neuroprotection versus neurotoxicity. Nat. Rev. Neurosci. 8, 766–775.

Costa, E.T., do-Nascimento, J.L., Picanço-Diniz, C.W., Quaresma, J.A., Silva-Filho, M., 1996. Histochemical characterization of NADPH-diaphorase activity in area 17 of diurnal and nocturnal primates and rodents. Braz. J. Med. Biol. Res. 29, 1355–1362.

Dawson, T.M., Bredt, D.S., Fotuhi, M., Hwang, P.M., Snyder, S.H., 1991. Nitric oxide synthase and neuronal NADPH diaphorase are identical in brain and peripheral tissues. Proc. Natl. Acad. Sci. U. S. A. 88, 7797–7801.

DeFelipe, J., Farinas, I., 1992. The pyramidal neuron of the cerebral cortex: morphological and chemical characteristics of the synaptic inputs. Prog. Neurobiol. 39, 563–607.

DeFelipe, J., Gonzalez-Albo, M.C., Del Rio, M.R., Elston, G.N., 1999. Distribution and patterns of connectivity of interneurons containing calbindin, calretinin, and parvalbumin in visual areas of the occipital and temporal lobes of the macaque monkey. J. Comp. Neurol. 412, 515–526.

de Lima, S.M., Ahnelt, P.K., Carvalho, T.O., Silveira, J.S., Rocha, F.A., Saito, C.A., Silveira, L.C.L., 2005. Horizontal cells in the retina of a diurnal rodent, the agouti (*Dasyprocta aguti*). Vis. Neurosci. 22, 707–720.

Douglas, R.J., Martin, K.A., Whitteridge, D., 1989. A canonical microcircuit for neocortex. Neural Comput. 1, 480–488.

Elston, G.N., 2002. Cortical heterogeneity: implications for visual processing and polysensory integration. J. Neurocytol. 31, 317–335.

Elston, G.N., 2003a. Cortex, cognition and the cell: new insights into the pyramidal neuron and prefrontal function. Cereb. Cortex 13, 1124–1138.

Elston, G.N., 2003b. Pyramidal cell heterogeneity in the visual cortex of the nocturnal New World owl monkey (*Aotus trivirgatus*). Neuroscience 117, 213–219.

Elston, G.N., 2007. Specializations in pyramidal cell structure during primate evolution. In: Kaas, J.H., Preuss, T. (Eds.), Evolution of Nervous Systems, 4. Academic Press, Oxford, pp. 191–242.

Elston, G.N., DeFelipe, J., 2002. Spine distribution in neocortical pyramidal cells: a common organizational principle across species. In: Azmitia, E.C., DeFelipe, J., Jones, E.G., Rakic, P., Ribak, C.E. (Eds.), Prog. Brain Res., 136. Elsevier, pp. 109–133.

Elston, G.N., Rockland, K.S., 2002. The pyramidal cell of the sensorimotor cortex of the macaque monkey: phenotypic variation. Cereb. Cortex 12, 1071–1078.

Elston, G.N., Rosa, M.G.P., 1998. Morphological variation of layer III pyramidal neurones in the occipitotemporal pathway of the macaque monkey visual cortex. Cereb. Cortex 8, 278–294.

Elston, G.N., Rosa, M.G.P., 2006. Ipsilateral corticocortical projections to the primary and middle temporal visual areas of the primate cerebral cortex: area-specific variations in the morphology of connectionally identified pyramidal cells. Eur. J. Neurosci. 23, 3337–3345.

Elston, G.N., Tweedale, R., Rosa, M.G., 1999a. Cellular heterogeneity in cerebral cortex: a study of the morphology of pyramidal neurones in visual areas of the marmoset monkey. J. Comp. Neurol. 415, 33–51.

Elston, G.N., Tweedale, R., Rosa, M.G., 1999b. Cortical integration in the visual system of the macaque monkey: large-scale morphological differences in the pyramidal neurons in the occipital, parietal and temporal lobes. Proc. Biol. Sci. 266, 1367–1374.

Elston, G.N., Benavides-Piccione, R., Elston, A., DeFelipe, J., Manger, P., 2005a. Pyramidal cell specialization in the occipitotemporal cortex of the Chacma baboon (*Papio ursinus*). Exp. Brain Res. 167, 496–503.

Elston, G.N., Benavides-Piccione, R., Elston, A., Manger, P., DeFelipe, J., 2005b. Pyramidal cell specialization in the

occipitotemporal cortex of the vervet monkey (*Cercopithecus pygerythrus*). NeuroReport 16, 967–970.
Elston, G.N., Elston, A., Casagrande, V.A., Kaas, J., 2005c. Areal specialization in pyramidal cell structure in the visual cortex of the tree shrew: a new twist revealed in the evolution of cortical circuitry. Exp. Brain Res. 163, 13–20.
Elston, G.N., Elston, A., Freire, M.A.M., Gomes-Leal, W., Pereira Jr., A., Silveira, L.C.L., Picanço-Diniz, C.W., 2006. Specialization of pyramidal cell structure in the visual areas V1, V2 and V3 of the South American rodent, *Dasyprocta primnolopha*. Brain Res. 1106, 99–110.
Estrada, C., DeFelipe, J., 1998. Nitric oxide-producing neurons in the neocortex: morphological and functional relationship with intraparenchymal microvasculature. Cereb. Cortex 8, 193–203.
Franca, J.G., do-Nascimento, J.L., Picanço-Diniz, C.W., Quaresma, J.A., Silva, A.L., 1997. NADPH-diaphorase activity in area 17 of the squirrel monkey visual cortex: neuropil pattern, cell morphology and laminar distribution. Braz. J. Med. Biol. Res. 30, 1093–1105.
Franca, J.G., Volchan, E., Jain, N., Catania, K.C., Oliveira, R.L., Hess, F.F., Jablonka, M., Rocha-Miranda, C.E., Kaas, J.H., 2000. Distribution of NADPH-diaphorase cells in visual and somatosensory cortex in four mammalian species. Brain Res. 864, 163–175.
Freire, M.A.M., Gomes-Leal, W., Carvalho, W.A., Guimarães, J.S., Franca, J.G., Picanço-Diniz, C.W., Pereira Jr., A., 2004. A morphometric study of the progressive changes on NADPH diaphorase activity in the developing rat's barrel field. Neurosci. Res. 50, 55–66.
Freire, M.A.M., Franca, J.G., Picanço-Diniz, C.W., Pereira Jr., A., 2005. Neuropil reactivity, distribution and morphology of NADPH diaphorase type I neurons in the barrel cortex of the adult mouse. J. Chem. Neuroanat. 30, 71–81.
Freire, M.A.M., Oliveira, R.B., Picanço-Diniz, C.W., Pereira Jr., A., 2007. Differential effects of methylmercury intoxication in the rat's barrel field as evidenced by NADPH diaphorase histochemistry. Neurotoxicology 28, 175–181.
Freire, M.A.M., Tourinho, S.C., Guimarães, J.S., Oliveira, J.L.F., Picanço-Diniz, C.W., Gomes-Leal, W., Pereira Jr., A., 2008. Histochemical characterization, distribution and morphometric analysis of NADPH diaphorase neurons in the spinal cord of the agouti. Front. Neuroanat. 2, 2 doi:10.3389/neuro.05.002.2008.
Freire, M.A.M., Guimarães, J.S., Gomes-Leal, W., Pereira Jr., A., 2009. Pain modulation by nitric oxide in the spinal cord. Front. Neurosci. 3, 175–181.
Gabbott, P.L., Jays, P.R., Bacon, S.J., 1997. Calretinin neurons in human medial prefrontal cortex (areas 24a,b,c, 32′, and 25). J. Comp. Neurol. 381, 389–410.
Gomes, F.L., Yamada, E.S., Silveira, L.C.L., 1998. Morphology, size, and distribution of the alpha retinal ganglion cells of the agouti, *Dasyprocta aguti*. Invest. Ophthalmol. Vis. Sci. 39, S563.
Gonchar, Y., Burkhalter, A., 1997. Three distinct families of GABAergic neurons in rat visual cortex. Cereb. Cortex 7, 347–358.
Gonzalez-Albo, M.C., Elston, G.N., DeFelipe, J., 2001. The human temporal cortex: characterization of neurons expressing nitric oxide synthase, neuropeptides and calcium binding proteins, and their glutamate receptor subunit profiles. Cereb. Cortex 11, 1170–1181.
Guimarães, J.S., Freire, M.A.M., Lima, R.R., Souza-Rodrigues, R.D., Costa, A.M., dos Santos, C.D., Picanço-Diniz, C.W., Gomes-Leal, W., 2009. Mechanisms of secondary degeneration in the central nervous system during acute neural disorders and white matter damage. Rev. Neurol. 48, 304–310.
Hope, B.T., Michael, G.J., Knigge, K.M., Vincent, S.R., 1991. Neuronal NADPH diaphorase is a nitric oxide synthase. Proc. Natl. Acad. Sci. U. S. A. 88, 2811–2814.
Horton, J.C., Adams, D.L., 2005. The cortical column: a structure without a function. Philos. Trans. R. Soc. Lond. B. Biol. Sci. 360, 837–862.
Jacobs, B., Scheibel, A.B., 2002. Regional dendritic variation in primate cortical pyramidal cells. In: Schüz, A., Miller, R. (Eds.), Cortical Areas: Unity and Diversity. Taylor and Francis, London, pp. 111–131.
Jelinek, H., Elston, G.N., Zietsch, B., 2005. Fractal analysis: pitfalls and revelations in neuroscience. In: Losa, G.A., et al. (Ed.), Fractals in Biology and Medicine. Birkhauser Verlag AG, Switzerland, pp. 85–94.
Kaas, J.H., 2005. From mice to men: the evolution of the large, complex human brain. J. Biosci. 30, 155–165.
Krubitzer, L., 2009. In search of a unifying theory of complex brain evolution. Ann. N.Y. Acad. Sci. 1156, 44–67.
Larkman, A.U., 1991a. Dendritic morphology of pyramidal neurones in the visual cortex of the rat: I. Branching patterns. J. Comp. Neurol. 306, 307–319.
Larkman, A.U., 1991b. Dendritic morphology of pyramidal neurones in the visual cortex of the rat: III. Spine distributions. J. Comp. Neurol. 306, 332–343.
Lund, J.S., Yoshioka, T., Levitt, J.B., 1993. Comparison of intrinsic connectivity in different areas of macaque monkey cerebral cortex. Cereb. Cortex 3, 148–162.
Luth, H.J., Hedlich, A., Hilbig, H., Winkelmann, E., Mayer, B., 1994. Morphological analyses of NADPH-diaphorase/nitric oxide synthase positive structures in human visual cortex. J. Neurocytol. 23, 770–782.
Mainen, Z.F., Sejnowski, T.J., 1996. Influence of dendritic structure on firing pattern in model neocortical neurons. Nature 382, 363–366.
Malach, R., 1994. Cortical columns as devices for maximizing neuronal diversity. Trends. Neurosci. 17, 101–104.
Matsubara, J.A., Chase, R., Thejomayen, M., 1996. Comparative morphology of three types of projection-identified pyramidal neurons in the superficial layers of cat visual cortex. J. Comp. Neurol. 366, 93–108.
Mel, B., 1999. Why have dendrites? A computational perspective. In: Stuart, G., Spruston, N., Häusser, M. (Eds.), Dendrites. Oxford Univ. Press, New York, pp. 271–289.
Mountcastle, V.B., 1997. The columnar organization of the neocortex. Brain 120 (Pt 4), 701–722.
Nelson, S., 2002. Cortical microcircuits: diverse or canonical? Neuron 36, 19–27.
Norris, P.J., Faull, R.L., Emson, P.C., 1996. Neuronal nitric oxide synthase (nNOS) mRNA expression and NADPH-diaphorase staining in the frontal cortex, visual cortex and hippocampus of control and Alzheimer's disease brains. Mol. Brain Res. 41, 36–49.
Oswaldo-Cruz, E., Picanço-Diniz, C.W., Silveira, L.C.L., 1985. Physiological optics of some Amazon rodents with contrasting life style. J. Physiol. 367, 18P.
Pereira, A., Freire, M.A.M., Bahia, C.P., Franca, J.G., Picanço-Diniz, C. W., 2000. The barrel field of the adult mouse SmI cortex as revealed by NADPH-diaphorase histochemistry. NeuroReport 11, 1889–1892.
Picanço-Diniz, C.W., Oliveira, H.L., Silveira, L.C.L., Oswaldo-Cruz, E., 1989. The visual cortex of the agouti (*Dasyprocta aguti*): architectonic subdivisions. Braz. J. Med. Biol. Res. 22, 121–138.
Picanço-Diniz, C.W., Silveira, L.C.L., de Carvalho, M.S., Oswaldo-Cruz, E., 1991. Contralateral visual field representation in area 17 of the cerebral cortex of the agouti: a comparison between the cortical magnification factor and retinal ganglion cell distribution. Neuroscience 44, 325–333.
Picanço-Diniz, C.W., Silveira, L.C.L., Oswaldo-Cruz, E., 1992. A comparative survey of magnification factor in V1 and retinal ganglion cell topography of lateral-eyed mammals. In: Lent, R. (Ed.), The visual system from genesis to maturity. Birkhauser, Boston, Massachusetts, USA, pp. 188–197.

Poirazi, P., Mel, B.W., 2001. Impact of active dendrites and structural plasticity on the memory capacity of neural tissue. Neuron 29, 779–796.
Preuss, T.M., 2000. What's human about the human brain. In: Gazzaniga, M.S. (Ed.), The New Cognitive Neurosciences. MIT Press, Cambridge, MA, pp. 1219–1234.
Rall, W., 1959. Branching dendritic trees and motoneuron membrane resistivity. Exp. Neurol. 1, 491–527.
Rall, W., 1989. Cable theory for dendritic neurons. In: Koch, C., Segev, I. (Eds.), Methods in neuronal modeling: from synapses to networks. MIT, Cambridge, MA, pp. 9–62.
Rall, W., Burke, R.E., Holmes, W.R., Jack, J.J., Redman, S.J., Segev, I., 1992. Matching dendritic neuron models to experimental data. Physiol. Rev. 72, S159–186.
Rocha, E.G., Santiago, L.F., Freire, M.A.M., Gomes-Leal, W., Lent, R., Houzel, J.C., Franca, J.G., Pereira Jr., A., Picanço-Diniz, C.W., 2007. Callosal axon arbors in the limb representations of the somatosensory cortex (SI) in the agouti (*Dasyprocta primnolopha*). J. Comp. Neurol. 500, 255–266.
Rocha, F.A., Ahnelt, P.K., Peichl, L., Saito, C.A., Silveira, L.C.L., De Lima, S.M., 2009. The topography of cone photoreceptors in the retina of a diurnal rodent, the agouti (*Dasyprocta aguti*). Vis. Neurosci. 26, 167–175.
Rothnie, P., Kabaso, D., Hof, P.R., Henry, B.I., Wearne, S.L., 2006. Functionally relevant measures of spatial complexity in neuronal dendritic arbors. J. Theor. Biol. 238, 505–526.
Sandell, J.H., 1986. NADPH diaphorase histochemistry in the macaque striate cortex. J. Comp. Neurol. 251, 388–397.
Santiago, L.F., Rocha, E.G., Freire, M.A.M., Lent, R., Houzel, J.C., Picanço-Diniz, C.W., Pereira Jr., A., Franca, J.G., 2007. The organizational variability of the rodent somatosensory cortex. Rev. Neurosci. 18, 283–294.
Scherer-Singler, U., Vincent, S.R., Kimura, H., McGeer, E.G., 1983. Demonstration of a unique population of neurons with NADPH-diaphorase histochemistry. J. Neurosci. Meth. 9, 229–234.
Schweitzer, L., Renehan, W.E., 1997. The use of cluster analysis for cell typing. Brain Res. Protoc. 1, 100–108.
Segev, I., 1998. Sound grounds for computing dendrites. Nature 393, 207–208.
Silveira, L.C.L., Picanço-Diniz, C.W., Oswaldo-Cruz, E., 1989. Distribution and size of ganglion cells in the retinae of large Amazon rodents. Vis. Neurosci. 2, 221–235.
Spruston, N., 2008. Pyramidal neurons: dendritic structure and synaptic integration. Nat. Rev. Neurosci. 9, 206–221.
Spruston, N., Stuart, G., Häusser, M., 1999. Dendritic integration. In: Stuart, G., Spruston, N., Häusser, M. (Eds.), Dendrites. Oxford Univ. Press, New York, pp. 231–270.
Stepanyants, A., Hof, P.R., Chklovskii, D.B., 2002. Geometry and structural plasticity of synaptic connectivity. Neuron 34, 275–288.
Stuart, G., Spruston, N., Sakmann, B., Hausser, M., 1997. Action potential initiation and backpropagation in neurons of the mammalian CNS. Trends Neurosci. 20, 125–131.
Szentagothai, J., 1975. The "module-concept" in cerebral cortex architecture. Brain Res. 95, 475–496.
Tao, Z., Van Gool, D., Lammens, M., Dom, R., 1999. NADPH-diaphorase-containing neurons in cortex, subcortical white matter and neostriatum are selectively spared in Alzheimer's disease. Dement. Geriatr. Cogn. Disord. 10, 460–468.
Thomas, E., Pearse, A.G., 1964. The solitary active cells. Histochemical demonstration of damage-resistant nerve cells with a TPN-diaphorase reaction. Acta Neuropathol. (Berl) 27, 238–249.
Vetter, P., Roth, A., Hausser, M., 2001. Propagation of action potentials in dendrites depends on dendritic morphology. J. Neurophysiol. 85, 926–937.
Vincent, S.R., Kimura, H., 1992. Histochemical mapping of nitric oxide synthase in the rat brain. Neuroscience 46, 755–784.
Wong-Riley, M., Anderson, B., Liebl, W., Huang, Z., 1998. Neurochemical organization of the macaque striate cortex: correlation of cytochrome oxidase with Na+K+ATPase, NADPH-diaphorase, nitric oxide synthase, and N-methyl-D-aspartate receptor subunit 1. Neuroscience. 83, 1025–1045.
Yan, X.X., Garey, L.J., 1997. Morphological diversity of nitric oxide synthesising neurons in mammalian cerebral cortex. J. Brain Res. 38, 165–172.